Scaling Up Temperature Cycling-Induced Deracemization by Suppressing Non-Stereoselective Processes

René R. E. Steendam* and Joop H. ter Horst

University of Strathclyde, EPSRC Centre for Innovative Manufacturing in Continuous Manufacturing and Crystallization (CMAC),
Strathclyde Institute of Pharmacy and Biomedical Sciences,
Technology and Innovation Centre, 99 George Street, Glasgow G1 1RD, United Kingdom

ABSTRACT

The scale-up of Temperature Cycling Induced Deracemization (TCID) of sodium bromate is feasible provided that two non-stereoselective processes are suppressed. Both non-stereoselective processes occur as a result of insufficient crystal breakage or attrition. In the absence of crystal breakage or attrition during the temperature cycles, large crystals emerge and the resulting small total crystal surface area is unable to sufficiently consume the supersaturation during cooling, resulting in non-stereoselective nucleation. This non-stereoselective process can be avoided by applying small temperature cycles involving small dissolving solid fractions. However, this leads to a slow deracemization rate. In addition, crystals undergo non-stereoselective agglomeration, which leads to the formation of large racemic agglomerates constructed of both chiral forms. To counteract their formation, secondary nucleation through crystal breakage was found to be a key requirement. At a large scale, a homogenizer was used to induce crystal breakage which, in combination with

temperature cycles, led to the removal of racemic agglomerates as well as a significant increase in the deracemization rate. Overusing the homogenizer, however, caused the enantiomeric excess increase to stop. Our experiments show the importance of secondary nucleation in TCID of sodium bromate. However, secondary nucleation is currently not incorporated in the TCID process models. In the presence of a sufficient amount of crystals at the highest temperature and careful use of the homogenizer, TCID leads to complete deracemization in volumes up to 1 L, demonstrating the potential to extend TCID to industrial applications.

INTRODUCTION

A key challenge in pharmaceutical manufacturing is obtaining one chiral form of a compound in preference over the other.[1] Crystallization is an efficient way to achieve chiral purification because the crystalline phase can induce a high level of chiral selectivity during crystal growth.[2-7] Viedma ripening in particular enables easy, fast and complete deracemization of chiral crystals.[8-10] During Viedma ripening, a suspension consisting of conglomerate crystals of both chiral forms is continuously ground. Crystal grinding, Ostwald ripening, stereospecific agglomeration and solute racemization drive the initial racemic mixture of enantiopure crystals to an end state in which all of the crystals are of the same chiral form.[9, 11, 12] The possibility to scale-up Viedma ripening up to about 500 mL demonstrates that solid-phase deracemization has the potential to be applied in industry.[13, 14]

Instead of crystal grinding, solid-state deracemization is also possible through temperature differences in time or location. It was found that boiling a slurry of sodium chlorate in water leads to complete solid-state deracemization without the need for grinding because of local temperature variations.[15] The effect of temporal temperature differences was investigated in more detail through the use of temperature cycles, involving heating, which partially

dissolves the crystals, and subsequent cooling, which induces crystal growth and possibly nucleation. These temperature cycles facilitate autocatalytic deracemization which is similar to Viedma ripening in absence of the vigorous grinding of crystals. Temperature cycling-induced deracemization (TCID) has been applied to various intrinsically chiral compounds,[16] which includes a compound that racemizes through a reversible reaction[6] and to a racemic compound that undergoes deracemization via its conglomerate-forming salt.[17] The speed of TCID can be increased if damped temperature cycles are applied, in which case the temperature swings ΔT are reduced as the enantiomeric excess E increases.[18] A different approach to TCID involves circulation of a suspension between a hot and a cold vessel, with an overall temperature difference of only 2.5 °C.[19] In this particular case the crystallizer volume was approximately 50 ml, which is the largest scale tested so far for TCID. It is therefore not yet known whether TCID can be scaled up to larger volumes.

The aim of this research is to establish whether TCID is feasible at larger scales up to 1L. Based on previous experiments and models, it is expected that scale-up of TCID would be possible by simply subjecting temperature cycles to larger suspension volumes. The effect of crystal breakage changes considerably upon scale-up and therefore this research allows the study of this effect on TCID for the first time. The model system used in this study is sodium bromate in water. Sodium bromate is chiral in the solid state but achiral in solution. It therefore resembles a chiral pharmaceutical compound that undergoes instant solution-phase racemization. An aqueous suspension of sodium bromate can undergo deracemization through Viedma ripening[20] but TCID of such a conglomerate-forming achiral compound remains unreported.

EXPERIMENTAL

General

Sodium bromate (≥99.5% purity and ≤0.5% insoluble material and metals) was purchased from Alfa Aesar and used as received. MilliQ water was used as the solvent. In all experiments, a total concentration of C = 455 mg/ml sodium bromate in water was used. The suspension temperature was measured using a Pt100 thermocouple. In some of the experiments an IKA T18 digital ULTRA-TURRAX homogenizer was used to break up larger particles. The homogenizer consists of a stagnant shaft with an internal blade that was set to rotate at 3000 rpm.

Experimental Setups

Three setups with different volumes and configurations were tested in this study (Figure 1). All three setups were connected to a Lauda ECO Silver thermostat bath.

Setup S was a small-scale setup which consisted of a thermostated 30 ml round-bottom flask containing a total solution volume of 20 ml. The stirring speed of the magnetic stirring bar (length 2.5 cm, Ø 1 cm) was set at 1100 rpm unless stated otherwise. Setup M was an intermediate-scale setup which consisted of a thermostated 500 ml flask with a total solution of 300 ml. The stirring speed of the magnetic stirrer bar (length 3.5 cm, Ø 1.5 cm) was set at 1100 rpm. Setup L was a large-scale setup consisted of a thermostated 1000 ml Radleys stirred-tank reactor with a total solution of 1000 ml. Setup L was equipped with three baffles and a three-bladed (length of blade 3 cm) overhead stirrer, which was set at 400 rpm.

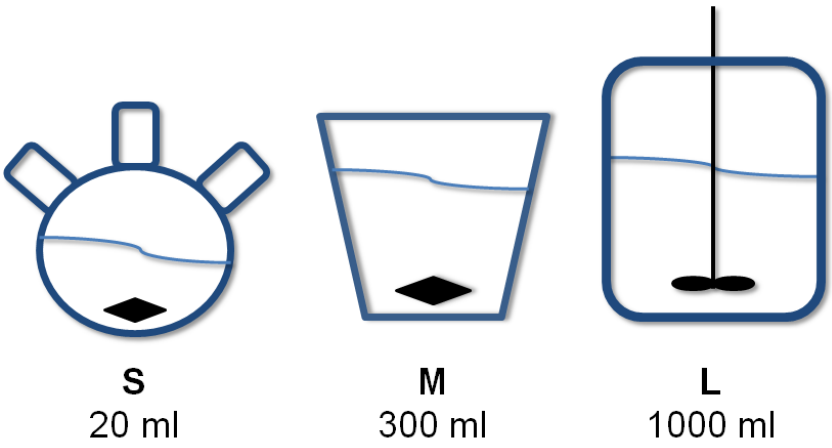

Figure 1. Schematic depictions of the three setups used in this study. Setup L was equipped with three baffles.

Temperature Cycling Experiments

Each experiment was started by setting the temperature of the reactor wall to T_{set} = 33 °C. After this, a 20 ml, 300 ml or a 1000 ml solid-free solution with a saturation temperature of T_{sus} = 33 °C and a concentration of C = 450 mg/ml was added to setup S, M or L, respectively. To setup S, M or L were added 0.1, 1.5 or 5 grams of crystals respectively after which the temperature of the reactor wall was set to T_{set} = 23 °C. The combination of solid-free solution and added crystals resulted in an overall concentration of C = 455 mg/ml. Once the suspension temperature T_{sus} reached 23 °C, stirring was commenced and a sample was taken to determine the enantiomeric excess E(0) at the start of the experiment. A temperature profile was repeatedly subjected to the suspension and samples were taken throughout the experiment during the first 5 minutes of a temperature cycle to determine the solid phase enantiomeric excess E. The different set temperature profiles used in this study are plotted in Figure 2.

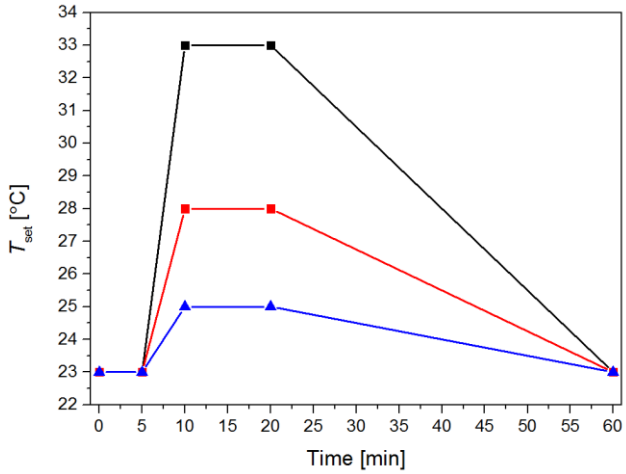

Figure 2. Set temperature profiles TP1 (black ●), TP2 (red ■) and TP3 (blue ▲) for a single temperature cycle. Temperature profiles TP1-3 each had a cycle time of one hour.

Temperature profiles TP1 to TP3 each took one hour to complete and the temperature cycles were repeated until the end of the experiment. Temperature profile TP4 and TP5 did not involve heating or cooling but remained at a constant temperature of T_{set} 23°C and 28°C respectively.

The temperature swing ΔT is defined as the difference between the highest measured suspension temperature T_{high} and the lowest measured suspension temperature T_{low}

$$\Delta T = T_{\text{high}} - T_{\text{low}} \quad (1)$$

The temperature T dependent solubility C^* of sodium bromate in water in mg/ml was previously determined using Crystal16 (Technobis) and can be described by the following linear fit[21]

$$C^*(T) = 248.00 + 6.12T \quad (2)$$

Assuming equilibrium, the solid mass fraction $f_{\Delta T}$ of the solids present at the lowest temperature T_{low} dissolving at the highest measured suspension temperature T_{high} in a temperature cycle was calculated through

$$f_{\Delta T} = \frac{C^*(T_{\mathrm{high}}) - C^*(T_{\mathrm{low}})}{C_t - C^*(T_{\mathrm{low}})} \quad (3)$$

in which $C^*(T_{high})$ is the saturation concentration in mg/ml at the highest measured suspension temperature T_{high} and $C^*(T_{low})$ is the solution concentration in mg/ml at the lowest measured suspension temperature T_{low} while C_t is the total dry mass concentration in mg/ml.[17] Then, the solid mass fraction w not dissolving at the highest measured suspension temperature T_{high} in a temperature cycle was determined by

$$w = 1 - f_{\Delta T} \quad (4)$$

Determination of the Enantiomeric Excess

During the experiments, small samples of the suspension were removed from the crystallizers using a pipette. Samples were taken at the point in the temperature cycle at which the temperature was at the lowest temperature T_{low}. The water was slowly evaporated from the samples at room temperature resulting in crystals that were sufficiently large allowing the chiral forms to be distinguished using a polarized microscope. Starting with crossed polarizers, turning the analyser clockwise resulted in l-crystals and d-crystals to become dark and bright respectively. Each sample contained a total of about 200 crystals and the number n_l and n_d of l- and d-crystals respectively were counted. Each sample was split up in three subsamples and for each subsample the enantiomeric excess E was determined through

$$E = \frac{n_d - n_l}{n_d + n_l} \quad (5)$$

This number based average enantiomeric excess E and standard error ΔE of the subsamples were calculated and used in this study.

RESULTS AND DISCUSSION

We first established the effect of the temperature cycles on the suspension temperature in both small and large scale setups. Next, small scale experiments (entry 1-3, Table 1) were tested which involve a temperature profile and reactor configuration similar to those reported elsewhere.[6, 16, 17] Scale-up experiments were tested by an intermediate scale experiment (entry 4, Table 1) and large scale experiments (entry 5-9, Table 1). Large scale experiments involving a homogenizer (entry 10-15, Table 1) are described and finally the implications of these results are discussed.

An overview of the tested experimental parameters is given in Table 1. Each deracemization experiment is denoted with a code constructed of an indication of the temperature programme (TP1 to TP5), of the small (S), medium (M) or large (L) setup used, and of the letter H indicating the use of a homogenizer. For example, the experiment involving temperature profile TP2 in the large setup L is designated as TP2-L.

Table 1. Overview of the process conditions during the experiments. Temperature profile TP, cycle time, small (S), medium (M) or large (L) setup used, stirring rate, use of homogenizer H, enantiomeric excess E(0) at time=0, temperature swing ΔT, mass fraction $f_{\Delta T}$ of solids that dissolves at the highest measured suspension temperature T_{high}, mass fraction w=1- $f_{\Delta T}$ of solids that does not dissolve at the highest temperature T_{high} in a temperature cycle and the cooling rate R_c.

Entry	Experiment	TP	Cycle Time [min]	Set up	Stirring Rate [rpm]	H	E(0)	ΔT [°C]	$f_{\Delta T}$	w	R_c [°C/min]
1	TP1-S1	1	60	S	1100	Off	0.06	8.0	0.74	0.26	0.21
2	TP1-S2	1	60	S	600	Off	0.07	8.0	0.74	0.26	0.21
3	TP4-S	4	-	S	1100	Off	0.02	0.0	0.00	1.00	0.00
4	TP1-M	1	60	M	1100	Off	0.09	9.4	0.88	0.12	0.24
5	TP1-L	1	60	L	400	Off	0.04	8.7	0.84	0.16	0.23
6	TP1-L1	1	60	L	400	Off	1.00	8.7	0.84	0.16	0.23
7	TP2-L1	2	60	L	400	Off	1.00	4.2	0.40	0.60	0.11
8	TP3-L1	3	60	L	400	Off	1.00	1.7	0.15	0.85	0.04
9	TP3-L	3	60	L	400	Off	0.15	1.7	0.15	0.85	0.04
10	TP1-LH	1	60	L	400	On	0.24	8.7	0.84	0.16	0.23
11	TP2-LH	2	60	L	400	On	0.15	4.2	0.40	0.60	0.11
12	TP3-LH	3	60	L	400	On	0.28	1.7	0.15	0.85	0.04
13	TP5-LH	5	-	L	400	On	0.50	0.0	0.00	1.00	0.00
14	TP2-LH1	2	60	L	400	On[a]	0.15	4.2	0.40	0.60	0.11
15	TP2-LH2	2	60	L	400	On[b]	0.15	4.2	0.40	0.60	0.11

[a]The homogenizer was switched off after N=50 temperature cycles. [b]The homogenizer was switched on after N=24 temperature cycles.

1. Temperature Cycling Conditions

The suspension temperatures T_{sus} during a single temperature cycle of the experiments TP1-S1, TP1-M and TP1-L and crystallizer wall temperature T_{cw} are plotted as a function of time in Figure 3a. The temperature of the water inside the crystallizer wall T_{cw} was equal to the set temperature T_{set} except for a small overshoot of 0.5 °C at the time that the highest temperature was reached. No temperature undershoot was measured after the cooling part of the cycle. The suspension temperatures T_{sus} did not reach the highest set temperature T_{set} between 10-25 minutes and this effect was most prominent for the small scale setup S. The cooling rates of the suspension temperatures T_{sus} were slightly lower than the cooling rates of the set temperature T_{set} for all tested volumes in combination with temperature profile TP1. The cooling rate R_c was determined from the slope of the linear fit of the cooling stage suspension temperature T_{sus} in time (Figure 3).

A crystallizer wall temperature T_{cw} which is significantly lower than the suspension temperature T_{sus} during cooling would result in local regions of high supersaturation near the reactor wall. As shown in Figure 3, the crystallizer wall temperature T_{cw} for the most part stays higher than the suspension temperature T_{sus} during cooling on a small scale S. During cooling at larger volumes the crystallizer wall temperature T_{cw} is approximately 1 °C lower than the suspension temperature T_{sus} towards the end of the cooling. Due to this local temperature difference, a high local supersaturation close to the crystallizer wall is expected.

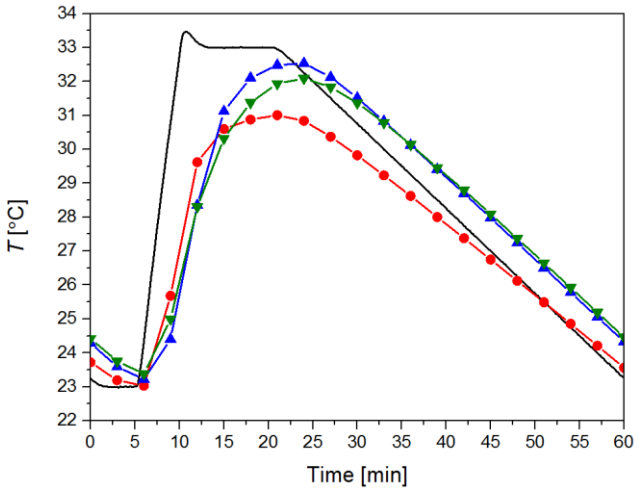

Figure 3. The crystallizer wall temperature (black line) and the suspension temperatures T_{sus} in experiments TP1-S (red ●), TP1-M (green ▼) and TP1-L (blue ▲) as a function of time for one temperature cycle. The cooling rate R_c of the set temperature T_{set} is 0.25 °C/min.

2. TCID on a Small Scale

The possibility of a sodium bromate suspension to undergo deracemization through temperature cycling was first tested in the small scale setup S of 20 ml. Experiment TP1-S1, in which the small scale setup S was used in combination with temperature profile TP1 using a stirring rate of 1100 rpm, led to the complete solid state deracemization within N=20 temperature cycles (Figure 4).

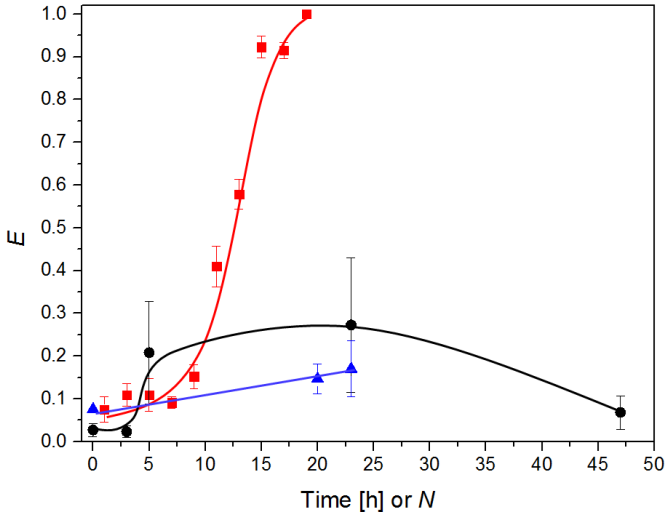

Figure 4. Enantiomeric excess E as a function of the number N of temperature cycles for small scale (20 ml) experiments TP1-S1 at a stirring rate of 1100 rpm (red ■), TP1-S2 at a stirring rate of 600 rpm (blue ▲) and TP4-S at a stirring rate of 1100 rpm without temperature swings ΔT (black ●). Each temperature cycle lasted 1 hour. The lines are a guide to the eye.

To exclude that the successful deracemization experiment (TP1-S1) was the result of Viedma ripening rather than temperature cycling, a constant temperature (T_{set} = 23 °C) experiment TP4-S was performed. After N=45 temperature cycles, the enantiomeric excess E < 0.1 (Figure 4). The enantiomeric excess E in experiment TP4-S appears to fluctuate over time, reaching levels up to roughly E=0.25 in which a small number of large crystals made the count-based analysis of the enantiomeric excess E less reliable. Nevertheless, it is clear that under isothermal Viedma ripening conditions no complete deracemization occurred.

To test the effect of the stirring rate, a small scale experiment was carried out with temperature profile TP1 but at a lower stirring speed of 600 rpm at which the crystals are still sufficiently suspended (TP1-S2). In this case, the enantiomeric excess E slightly increased from E=0.07 to E=0.15 after N=24 temperature cycles (Figure 4). Upon closer inspection of the crystalline product it was found that fewer but larger crystals were present as compared to

the TCID experiment at higher stirring speed. It is surprising that the stirring speed in a well suspended suspension has such a profound influence on the deracemization rate which leaves us to explore whether stirrer-induced stereoselective secondary nucleation or attrition may be an essential process in TCID.

3. Toward TCID on Larger Scales

After the successful TCID on a small scale, TCID was tested in a 300 ml suspension (Medium scale setup M) using temperature profile TP1 (TP1-M) and a 1L suspension (large scale setup L) with temperature profile TP1 (TP1-L). Under these conditions, no deracemization occurred and even after N=40 temperature cycles no significant increase in enantiomeric excess E was observed (Figure 5). In both large scale experiments, no increase but rather a small decrease from slightly enantiomerically-enriched to racemic crystals was observed. Apparently the scale up conditions lack or introduce a mechanism that prevents the deracemization.

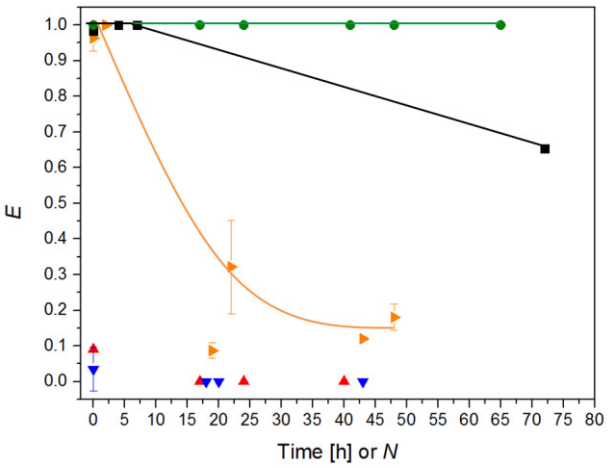

Figure 5. Enantiomeric excess E as a function of the number N of temperature cycles. Experiments TP1-M (red ▲) and TP1-L (blue ▼) starting with a low initial enantiomeric excess E(0) <0.1. Experiments TP1-L1, w=0.16 (orange ►), TP2-L1, w=0.60 (black ■) and TP3-L1, w=0.85 (green ●) starting with a high initial enantiomeric excess E(0)=1 and varying

weight fractions w of solids at T_{high}. Each temperature cycle lasted 1 hour. The lines are a guide to the eye.

In order to establish whether nucleation other than stereoselective secondary nucleation is responsible for the absence of deracemization on a larger scale, a suspension of 1L containing chirally pure crystals with E = 1 in Setup L was subjected to temperature profile TP1 (TP1-L1, Figure 5). The initial enantiomeric excess E(0) started to decrease after only a few temperature cycles. Due to the relative small weight fraction w=0.12 of solids left at T_{high} in the cycle, high levels of supersaturation are present during the fast cooling with a rate R_c of 0.23 °C/min from the high to the low temperature. The small amount of crystals apparently could not sufficiently deplete the applied supersaturation either by growth or by inducing stereoselective secondary nucleation during the fast cooling stage. Instead, non-stereoselective nucleation must have repeatedly occurred which led to a drive towards a racemic composition in the solid phase. Based on the temperature differences observed between the crystallizer wall and the suspension temperature (Figure 3), such a non-stereoselective nucleation process could occur at the crystallizer wall at which, during cooling, the supersaturation locally is higher than that in the bulk. A local high level of supersaturation at the crystallizer wall facilitates heterogeneous nucleation which is commonly observed in heat-exchange crystallization processes[22] including in our previous study involving the continuous cooling crystallization of sodium bromate.[21]

The time at which non-stereoselective nucleation occurred could be extended by using a temperature profile involving smaller temperature swings ΔT (Figure 5). Through our definition of the temperature profile at which the lower temperature is unchanged, such smaller temperature swings ΔT result in larger fractions w of solids present at T_{high}. During cooling a larger crystal mass is available for growth and stirrer-induced stereoselective

secondary nucleation avoids non-stereoselective nucleation close to the crystallizer wall. Compared to TP1-L1 in which the weight fraction w=0.2 of solids at T_{high}=32.1 °C is low, experiment TP2-L1 involved a three times higher weight fraction w=0.6 of solids at T_{high}=27.4 °C. During experiment TP2-L1, this prevented non-stereoselective nucleation from occurring in the first N=10 temperature cycles, as indicated by the slower decrease in enantiomeric excess E over time (Figure 5).

Starting with an enantiopure E=1 suspension in experiment TP3-L1, non-stereoselective nucleation was completely inhibited over the course of N=65 temperature cycles. In this experiment a relative large weight fraction w=0.9 of solids at T_{high}=24.7 °C was present which probably induced a sufficient amount of growth and a high degree of stereoselective secondary nucleation to maintain enough crystal surface to prevent non-stereoselective nucleation. In order to prevent non-stereoselective nucleation the amount of crystals at T_{high} should therefore be sufficiently large. In the case of sodium bromate under the experimental conditions in this research the lower boundary for the weight fraction w at T_{high} lies between 0.6 and 0.9.

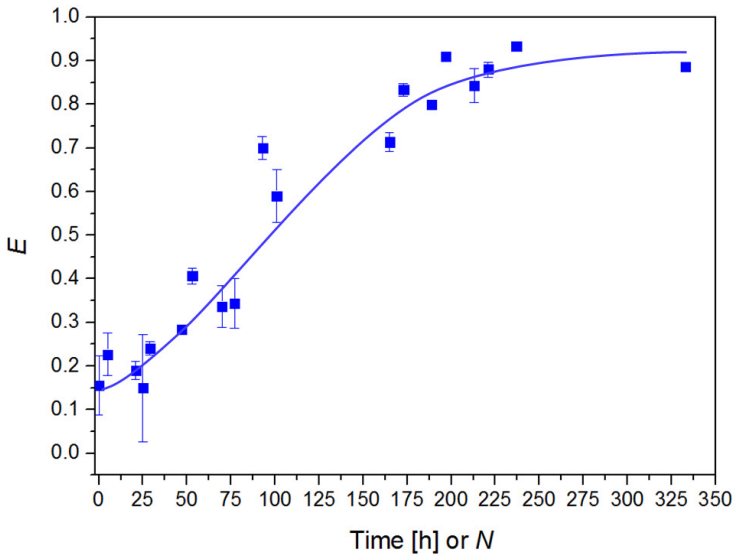

Figure 6. Enantiomeric excess E as a function of the number N of temperature cycles during experiment TP3-L conducted in Setup L in combination with temperature profile TP3 using a weight fraction w=0.9 at T_{high}=24.7 °C. Each temperature cycle lasted 1 hour. The line is a guide to the eye.

Thus non-stereoselective nucleation could be inhibited provided that a sufficiently large weight fraction of solids was present at the highest temperature of the temperature cycle. To determine whether such conditions would lead to TCID, experiment TP3-L was tested with a large weight fraction w=0.9 of solids at T_{high} and a temperature profile TP3 on a 1L scale using an initial enantiomeric excess E(0)=0.15. This experiment led to partial deracemization up to an enantiomeric excess E of 0.9 (Figure 6). However, the deracemization rate was very slow as it took more than N=200 temperature cycles to achieve this enantiomeric excess. In addition, a further increase above E=0.9 could not be realized. Upon inspection of crystalline samples this was attributed to the presence of a small amount of large racemic agglomerates. Both chiral forms are present in what appear to be large single crystals consisting of chirally pure regions (Figure 7).

Apparently, during the cooling part of the temperature cycling the applied supersaturation induced non-stereoselective agglomeration. In this process the tetrahedral-shaped crystals agglomerate to give large crystals that also adopt a tetrahedral shape. Due to their large size, these agglomerates do not dissolve during the heating part of the cycle, preventing full deracemization.

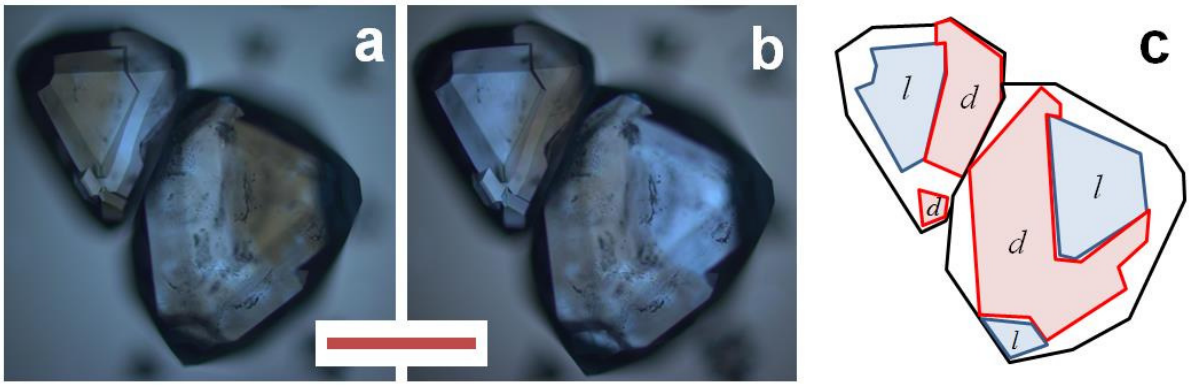

Figure 7. The left two images are polarised microscope images of crystals which were sampled from a slurry which was subjected to N=20 temperature cycles using TP-1 in setup C. The different chiral regions can be distinguished by their corresponding different colours (brown and blue). a) Analyser turned clockwise. b) Analyser turned counter clockwise. c) Schematic representation of the microscope images in which the chirality of the crystals is identified. Some of the parts of the crystals are not coded as it was unclear by microscopy to identify the chirality. The scale bar represents 500 µm.

The agglomeration of sodium bromate in saturated boiling solutions was investigated by Viedma et al.[23] In their experiments, the majority of the agglomerates consisted of the same chiral form. Although chiral misalignment also occurred in their isothermal experiments, the racemic agglomerates were observed to break and re-agglomerate to enantiopure agglomerates. In our experiments on the other hand, any chiral misalignment would be captured during the cooling step of a temperature cycle. After cooling, the large recrystallized racemic agglomerates survive the heating steps during subsequent temperature cycles and therefore our experiments failed to undergo complete TCID. In Viedma ripening type processes involving grinding, such large agglomerates would be broken up to smaller crystals which in TCID less readily will happen. Therefore, in order to achieve full deracemization in TCID, the formation of these racemic agglomerates should be avoided or counterbalanced.

4. Achieving Full TCID on a Large Scale

In TCID crystal breakage is required to remove any large racemic crystal agglomerates. To induce crystal breakage in our large scale TCID experiments, it was chosen to use a homogenizer. A homogenizer consists of a rapidly rotating blade of about 1 cm that rotates at 3000 rpm within a stagnant shaft. Crystals entering the shaft are crushed into smaller particles. It is expected that the homogenizer impacts the entire crystal population and therefore also breaks large racemic agglomerates into smaller, possibly enantiopure crystals. Apart from removing the racemic agglomerates, reducing the crystal size is also expected to increase the deracemization rate.

In principle, the grinding effect of the homogenizer could also induce Viedma ripening. However, we have previously shown that the effect of a homogenizer alone was insufficient to induce Viedma ripening at room temperature on a 1 litre scale in our continuous crystallization experiments.[21] To also rule out the occurrence of Viedma ripening due to a homogenizer in a batch-wise process, a Viedma ripening experiment was carried out using a constant temperature T of 28 °C and with a homogenizer (TP5-LH), starting at an initial enantiomeric excess E of about 0.5. As expected, no Viedma ripening was observed as the enantiomeric excess E remained unchanged, even after 70 hours.

To test whether the use of a homogenizer would lead to full TCID on a large scale, temperature profile TP3 was applied to a suspension with a weight fraction w=0.9 at T_{high} in the large scale setup L using a homogenizer (TP3-LH). In this experiment, close to complete deracemization (E=0.98) was achieved after 40 hours (Figure 8a). Visual inspection of the crystal samples did not show any racemic agglomerates. As expected, the homogenizer removes large racemic agglomerates which otherwise would inhibit the deracemization process. In addition, the deracemization rate greatly increased compared to the same

experiment without the homogenizer (TP3-L) in which more than 5 times more temperature cycles were needed to arrive at the same change in enantiomeric excess E (Figure 6).

In experiment TP2-LH, a mass fraction of solids w=0.6 present at T_{high}=27.4 °C also led to deracemization but up to a final enantiomeric excess of about E=0.87 at which no further increase in E was observed. In experiment TP1-LH with w=0.2, partial deracemization was achieved as well but the final enantiomeric excess was about E=0.75 as it stopped to increase after about 22 cycles.

Interestingly the mass fraction w of solids does not seem to substantially influence the TCID rate. Possibly a maximum deracemization rate was already achieved in experiment TP3-LH involving the highest tested mass fraction w=0.9 of solids. It seems that the rate of deracemization is mainly dependent on the degree of stereoselective secondary nucleation whereas the temperature swings ΔT or cooling rates R_c that are part of the temperature profile appear to have a negligible effect on the deracemization rate.

Although a high deracemization rate could be achieved with temperature cycles in combination with the homogenizer, still no full deracemization could be obtained although the final enantiomeric excess E increases towards 1 at larger w as shown in Figure 8b. The levelling off of the enantiomeric excess E prevents complete deracemization and seems to indicate that again racemic agglomerates are present, similar to those in experiment TP-1. However, close inspection of the crystal samples showed no indication of racemic crystals. Instead, the homogenizer could have led to the formation of monodispersed crystals. It was shown that a monodisperse size distribution during a deracemization process is responsible for the levelling off of the enantiomeric excess E.[24]

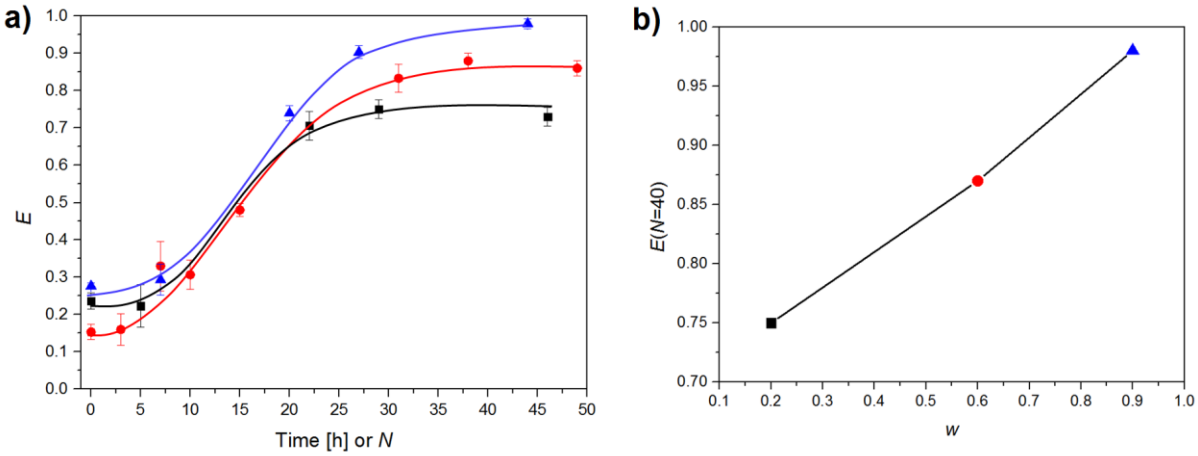

Figure 8. Experiments in setup L with the homogenizer. a) Enantiomeric excess E as a function of time for experiments TP1-LH, w=0.2 (black ■), TP2-LH, w=0.6 (red ●) and TP3-LH, w=0.9 (blue ▲). b) The enantiomeric excess E after N=40 temperature cycles for TP1-LH (black ■), TP2-LH (red ●) and TP3-LH (blue ▲) plotted as a function of the mass fraction of solids w present at T_{high}. The lines are a guide to the eye.

To test that monodispersity is responsible for the levelling off of the enantiomeric excess E in experiment TP2-LH, we switched off the homogenizer in that experiments after N=50 temperature cycles (experiment TP2-LH1, Figure 9). In the absence of the operating homogenizer the crystal size distribution could develop away from monodispersity and the suspension started to deracemize again. We thus found that the enantiomeric excess E=0.87 obtained in experiment TP2-LH could be increased to E=1.0.

Complete deracemization was also achieved in experiment TP2-LH2 in which the homogenizer was switched on only after N=25 temperature cycles (Figure 9). During the first N=25 temperature cycles large racemic single crystals were formed and the enantiomeric excess E did not increase. However, immediately after switching on the homogenizer after N=25 temperature cycles the enantiomeric excess E started to increase and complete TCID was achieved. The large crystals that were initially formed within the first N=25 temperature

cycles were possibly far away from being monodisperse. The time required to make these large crystals monodisperse probably exceeded the time required for complete deracemization.

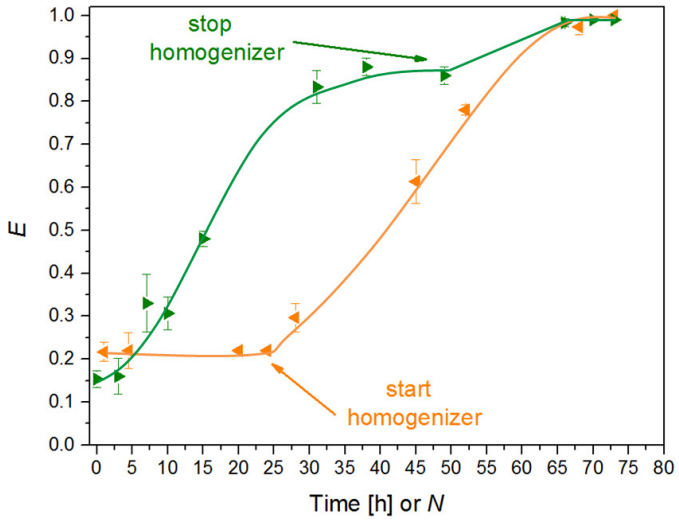

Figure 9. Enantiomeric excess E as a function of the number N of temperature cycles for different experiments in setup L with the temporary presence of a homogenizer at a solid fraction of w=0.6 at T_{high}=27.4°C. TP2-LH1 in which the homogenizer was switched on after N=24 temperature cycles (orange ◄) and TP2-LH1 in which the homogenizer was switched off after N=50 temperature cycles (green ►). Each temperature cycle lasted 1 hour. The lines are a guide to the eye.

DISCUSSION

In order to achieve full Temperature Cycling Induced Deracemization (TCID) two non-stereoselective inhibiting processes must be avoided. The first process that inhibits TCID is non-stereoselective nucleation as it leads to the formation of both chiral forms. Non-stereoselective nucleation likely proceeds during cooling through heterogeneous nucleation on or close to the cold surface of the crystallizer wall where the local supersaturation would be higher than the bulk supersaturation. For larger scale processes the local supersaturations

at the heat exchanger surfaces are often higher because of the larger amount of heat to be exchanged, increasing the probability of non-stereoselective nucleation. Non-stereoselective nucleation can be avoided by increasing the mass fraction w of solids at T_{high} which results in a larger fraction of solids available for growth. However, to speed-up and achieve full TCID a high level of crystal grinding and attrition is required so that new small fragments are available to dissolve during every temperature cycle. At large scales a method additional to stirring is required to induce stereoselective secondary nucleation and we showed that a homogenizer is suitable to achieve this. For smaller scales, stirrer-induced crystal breakage seems sufficient to induce stereoselective secondary nucleation.

The second process that inhibits TCID is non-stereoselective agglomeration as it leads to the formation of large racemic crystals. Due to their large sizes, the racemic crystals do not undergo dissolution during heating and therefore deracemization cannot be achieved using temperature cycles alone. At large scales an additional method to stirring, such as a homogenizer, is needed to break the racemic crystals. On a small scale, stirrer-induced crystal breakage is typically enough to break the large racemic crystals.

In addition to non-stereoselective processes, TCID can be inhibited due to the formation of monodispersed crystals, which in our experiments were formed due to the prolonged use of the homogenizer. To achieve complete deracemization, the crystals need to move away from being monodisperse. This can be realized by switching off the homogenizer when crystals become monodisperse which is when the enantiomeric excess E stops to increase. Alternatively, temperature cycles can be used to initially create large racemic crystals that are sufficiently far away from being monodisperse. The time needed to make these large racemic crystals monodisperse must be longer than the time required for complete TCID. A possible strategy to avoid the emergence of monodisperse crystals could be to use the homogenizer only during the cooling parts of the temperature profile. Finally, in addition to switching the

homogenizer on or off during TCID, further deracemization might be realized if large enantiopure seed crystals are added to the suspension.[24]

Up to now only small scale TCID experiments with volumes up to 50 mL have been investigated. In these TCID experiments secondary nucleation was not identified, probably due to the difficulty of monitoring crystal size distribution during such small scale processes. Therefore, stereoselective secondary nucleation was not incorporated in the models to explain previously reported experiments.[25-27] However, as we have shown herein that stereoselective secondary nucleation is a key requirement to achieve TCID.

CONCLUSIONS

Here we showed that temperature cycling induced deracemization (TCID) can be achieved on larger scales. Two non-stereoselective processes were observed that could inhibit TCID: non-stereoselective nucleation and non-stereoselective agglomeration. Furthermore, a monodisperse suspension could prevent complete TCID. By overcoming these inhibiting processes using tailored process conditions, we have established the scale-up of TCID, a step towards implementing TCID as an industrial process. More importantly, this contribution indicates that stereoselective secondary nucleation is an essential process in TCID, substantially increasing its rate. So far, these inhibiting processes have not been recognized in other TCID experiments but their mechanisms and roles have to be understood in order to enable the construction of accurate TCID process models and to optimize the TCID processes.

AUTHOR INFORMATION

Corresponding Author

* E-mail: renesteendam@gmail.com

Notes

The authors declare no competing financial interest.

ACKNOWLEDGEMENTS

We thank Iqra Irfan for carrying out part of the experimental work. This work is part of the research program Rubicon with project number 2015/00910/N, which is financed by the Netherlands Organization for Scientific Research (NWO). The authors thank the EPSRC Centre for Innovative Manufacturing in Continuous Manufacturing and Crystallisation (http://www.cmac.ac.uk) for supporting this work (EPSRC funding under grant reference: EP/I033459/1).

REFERENCES

(1) Balzani, V.; Meijere, A. d.; Houk, K. N.; Kessler, H.; Lehn, J. M.; Ley, S. V.; Schreiber, S. L.; Thiem, J.; Trost, B. M.; Vögtle, F.; Yamamoto, H., Topp. Curr. Chem. **2007,** 269, 1-313.
(2) Viedma, C.; Coquerel, G.; Cintas, P., Handbook of Crystal Growth, Elsevier, 2015
(3) Lorenz, H.; Seidel-Morgenstern, A., Angew. Chem. Int. Ed. **2014,** 53, 1218-1250.
(4) Xiouras, C.; Ter Horst, J. H.; Van Gerven, T.; Stefanidis, G. D., Cryst. Growth Des. **2017,** 17, 4965-4976.
(5) Xiouras, C.; Van Cleemput, E.; Kumpen, A.; ter Horst, J. H.; Van Gerven, T.; Stefanidis, G. D., Cryst. Growth Des. **2016,** 17, 882-890.
(6) Steendam, R. R. E.; van Benthem, T. J. B.; Huijs, E. M. E.; Meekes, H.; van Enckevort, W. J. P.; Raap, J.; Rutjes, F. P. J. T.; Vlieg, E., Cryst. Growth Des. **2015,** 15, 3917-3921.
(7) Steendam, R. R. E.; Verkade, J. M. M.; van Benthem, T. J. B.; Meekes, H.; van Enckevort, W. J. P.; Raap, J.; Rutjes, F. P. J. T.; Vlieg, E., Nat. Commun. **2014,** 5, 10.1038/ncomms6543.
(8) Viedma, C., Phys. Rev. Lett. **2005,** 94, 065504-1-065504-4.
(9) Noorduin, W. L.; Meekes, H.; Bode, A. A. C.; van Enckevort, W. J. P.; Kaptein, B.; Kellogg, R. M.; Vlieg, E., Cryst. Growth Des. **2008,** 8, 1675-1681.
(10) Sogutoglu, L.-C.; Steendam, R. R. E.; Meekes, H.; Vlieg, E.; Rutjes, F. P. J. T., Chem. Soc. Rev. **2015,** 44, 6723-6732.
(11) Iggland, M.; Mazzotti, M., CrystEngComm **2013,** 15, 2319-2328.
(12) Noorduin, W. L.; van Enckevort, W. J. P.; Meekes, H.; Kaptein, B.; Kellogg, R. M.; Tully, J. C.; McBride, J. M.; Vlieg, E., Angew. Chem. Int. Ed. **2010,** 49, 8435-8438.
(13) Noorduin, W. L.; van der Asdonk, P.; Bode, A. A. C.; Meekes, H.; van Enckevort, W. J. P.; Vlieg, E.; Kaptein, B.; van der Meijden, M. W.; Kellogg, R. M.; Deroover, G., Org. Process Res. Dev. **2010,** 14, 908-911.

(14) Iggland, M.; Fernández-Ronco, M. P.; Senn, R.; Kluge, J.; Mazzotti, M., Chem. Eng. Sci. **2014,** 111, 106-111.
(15) Viedma, C.; Cintas, P., Chem. Commun. **2011,** 47, 12786-12788.
(16) Suwannasang, K.; Flood, A. E.; Rougeot, C.; Coquerel, G., Cryst. Growth Des. **2013,** 13, 3498-3504.
(17) Li, W. W.; Spix, L.; de Reus, S. C. A.; Meekes, H.; Kramer, H. J. M.; Vlieg, E.; ter Horst, J. H., Cryst. Growth Des. **2016,** 16, 5563-5570.
(18) Suwannasang, K.; Flood, A. E.; Rougeot, C.; Coquerel, G., Org. Proc. Res. & Dev. **2017,** 21, 623-630.
(19) Suwannasang, K.; Flood, A. E.; Coquerel, G., Cryst. Growth Des. **2016,** 16, 6461-6467.
(20) Viedma, C., Cryst. Growth Des. **2007,** 7, 553-556.
(21) Steendam, R. R. E.; ter Horst, J. H., Cryst. Growth Des. **2017,** 17, 4428-4436.
(22) Narducci, O.; Jones, A. G.; Kougoulos, E., Chem. Eng. Sci. **2011,** 66, 1069-1076.
(23) Viedma, C.; McBride, J. M.; Kahr, B.; Cintas, P., Angew. Chem. Int. Ed. **2013,** 52, 10545-10548.
(24) Xiouras, C.; Van Aeken, J.; Panis, J.; Ter Horst, J. H.; Van Gerven, T.; Stefanidis, G. D., Cryst. Growth Des. **2015,** 15, 5476-5484.
(25) Suwannasang, K.; Coquerel, G.; Rougeot, C.; Flood, A. E., Chem. Eng. Technol. **2014,** 37, 1329-1339.
(26) Uchin, R.; Suwannasang, K.; Flood, A. E., Chem. Eng. Technol. **2017,** 40, 1252-1260.
(27) Katsuno, H.; Uwaha, M., Phys. Rev. E **2016,** 93, 013002.

TOC Graphic

Scaling Up Temperature Cycling-Induced Deracemization by Suppressing Non-Stereoselective Processes

René R. E. Steendam* and Joop H. ter Horst

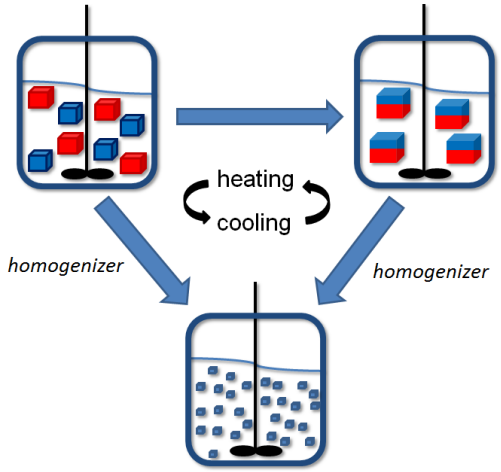

The scale-up of Temperature Cycling Induced Deracemization (TCID) of sodium bromate is feasible provided that non-stereoselective nucleation and non-stereoselective agglomeration are suppressed. Stereoselective secondary nucleation is a key requirement to achieve TCID.